Computing in High-Energy and Nuclear Physics
(Mumbai, India – February 13-17, 2006)

Update On the Status of the FLUKA Monte Carlo Transport Code*

A. Ferrari, M.Lorenzo-Sentis, S. Roesler, G. Smirnov, F.Sommerer, C.Theis and V.Vlachoudis, CERN, Geneva, Switzerland

M. Carboni, A. Mostacci, M. Pelliccioni and R. Villari, INFN, Frascati, Italy

V. Anderson, N. Elkhayari, A. Empl, K. Lee, B. Mayes, L. Pinsky* and N. Zapp
Physics Department, University of Houston, Houston, TX 77204-5005, USA

K. Parodi, H. Paganetti and T. Bortfeld, Massachusetts General Hospital,
Department of Radiation Oncology, Boston, MA, 02114 USA

G. Battistoni, M. Campanella, F. Cerutti, P. Colleoni, E. Gadioli, M.V. Garzelli, M. Lanza, S.Muraro, A. Pepe and P. Sala, INFN and Univ. of Milan, Italy

T. L. Wilson. NASA/JSC, Houston, TX, 77058 USA

D. Alloni, F. Ballarini, M. Liotta, A. Mairani, A. Ottolenghi, D. Scannicchio and S. Trovati, INFN and Univ. Pavia, Italy

J. Ranft, Siegen Univ., Germany

A. Fasso', SLAC, USA

Abstract

The FLUKA Monte Carlo transport code is a well-known simulation tool in High Energy Physics. FLUKA is a dynamic tool in the sense that it is being continually updated and improved by the authors. We review the progress achieved since the last CHEP Conference on the physics models, some technical improvements to the code and some recent applications. From the point of view of the physics, improvements have been made with the extension of PEANUT to higher energies for p, n, pi, pbar/nbar and for nbars down to the lowest energies, the addition of the online capability to evolve radioactive products and get subsequent dose rates, upgrading of the treatment of EM interactions with the elimination of the need to separately prepare preprocessed files. A new coherent photon scattering model, an updated treatment of the photo-electric effect, an improved pair production model, new photon cross sections from the LLNL Cullen database have been implemented. In the field of nucleus--nucleus interactions the electromagnetic dissociation of heavy ions has been added along with the extension of the interaction models for some nuclide pairs to energies below 100 MeV/A using the BME approach, as well as the development of an improved QMD model for intermediate energies. Both DPMJET 2.53 and 3 remain available along with rQMD 2.4 for heavy ion interactions above 100 MeV/A. Technical improvements include the ability to use parentheses in setting up the combinatorial geometry, the introduction of pre-processor directives in the input stream. a new random number generator with full 64 bit randomness, new routines for mathematical special functions (adapted from SLATEC). Finally, work is progressing on the deployment of a user-friendly GUI input interface as well as a CAD-like geometry creation and visualization tool. On the application front, FLUKA

has been used to extensively evaluate the potential space radiation effects on astronauts for future deep space missions, the activation dose for beam target areas, dose calculations for radiation therapy as well as being adapted for use in the simulation of events in the ALICE detector at the LHC.

Current FLUKA Status

This paper presents an update to the report presented at the CHEP-2004 [1]. The currently available release of FLUKA, designated FLUKA2005.6, (for which download, including the source code under a license, is now available; see http://www.fluka.org for the details), has seen extensive scientific and technical improvements over the last official major version release. These include:

…for the scientific improvements:

a) The online time evolution of radioactive products and associated remnant dose calculation capability has been added.

b) The extension of PEANUT, FLUKA's intermediate energy nuclear interaction event generator, to cover pbar/nbar and, the elimination of Nucriv for p, n, pi's, pbar/nbar. Among the many consequences of this development is that the threshold for nbar transport and interactions can now be set as low as the user wishes. This advance presages the eventual retirement of the oldest and least reliable part of the hadronic interaction models.

c) ElectroMagnetic dissociation of heavy ions is now incorporated.

d) The need to produce external preprocessed files as part of the electromagnetic initialization has now been removed, with that function being embedded within the normal FLUKA initialization process and the upgrading of the EM code to make it fully coherent with the general hadronic treatment within FLUKA.

e) New photon cross sections have been included based on the Cullen EPDL97 LLNL database [2].

f) A new photon coherent scattering model has been included with updated atomic form factors. Rayleigh scattering has been reworked from scratch with a novel approach.

g) The photon photoelectric effect model has been updated with individual edges now accounted for down to eV's

h) The photon pair production model has been updated, and now accounts for electron/positron asymmetries at low energies, as well as for departures from the plain Bethe-Heitler formalism. The procedure has been completely reworked using an approach which can distinguish between interactions in the nuclear or electron field, and properly samples the element in a compound or mixture on which the interaction is going to occur. The new algorithm is also capable of producing meaningful results for photon energies close to thresholds, where several corrections are important and the symmetry electron/positron is broken, in similar fashion to the bremsstrahlung case.

i) Introduction of a new fragmentation model which improves the performance with respect to the residual nuclei.

…and the following technical changes in the code:

l) The ability to use parentheses in setting up the combinatorial geometry (available, but not included in the release yet)

m) The introduction of (simple) preprocessed directives in the input stream.

n) A new random number generator with full 64 bit randomness based on the latest suggestions from G. Marsaglia and W.W Tsang [3] has been implemented.

o) New routines for mathematical special functions (adapted from SLATEC)

p) Interface with DPMJET-3 (the interface with DPMJET-2.53 is also still available)

In addition, the following projects are currently under active development. Some of them are ready but were not included for lack of time, others are ready, but not yet tested enough for a general user version, others are in various stages of completeness.

a) New 260 group neutron cross section library

b) Heavy fragment emission in the preequilibrium stage

c) Impact ionization cross sections

d) Compton with Doppler shift

e) PEANUT extension to the highest energies by incorporating into its sophisticated nuclear framework the Glauber cascade and DPM part of the high energy model.

f) Heavy ion pair production

g) Photomuon production

h) Full input by names rather than numbers

i) Direct resonance transport and interaction in PEANUT

j) Updated multiple scattering model (including the so-called polygonal approach)

k) New hadron elastic scattering model at intermediate energies

l) Neutral kaon regeneration (partially implemented, but still faulty because not yet performed at scattering amplitude level)

m) Screening and Coulomb corrections for the spectra of the decay beta minus and beta plus emissions

Activation and Dose Evolution

The possibility to compute online the time evolution of a radionuclide inventory has been added, with an exact analytical implementation (Bateman equations) of the activity evolution during irradiation and cooling down.

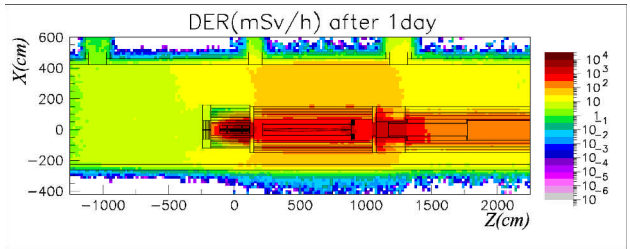

1a

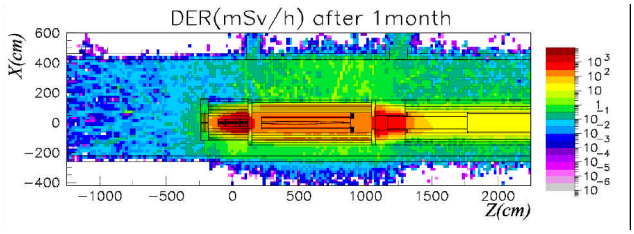

1b

Figure 1. The residual Dose Equivalent Rate (DER) due to the evolution of the activation is shown for the CNGS neutrino facility in the hottest area (target/magnetic horn) at 1 day (a) and 1 month (b).

Furthermore, the generation and transport of decay radiation is now possible. A dedicated database of decay emissions has been created using mostly information obtained from NNDC, supplemented in some cases with other data and checked for consistency. As a consequence, results for production of residuals, their time evolution and residual doses due to their decays can now be obtained in the same run for an arbitrary number of decay times and for a given, arbitrarily complex, irradiation profile. Figure 1 shows the results of a calculation of the Dose Equivalent Rates one day and one month after irradiation. They represent the map of residual dose rates at different cooling times for the CNGS neutrino facility in the hottest area (target/magnetic horn).

Heavy Ion Event Generator Status

The currently available version of FLUKA, FLUKA2005.6, like recent prior versions include embedded comprehensive heavy ion event generators to simulate nucleus-nucleus inelastic interactions from 100 MeV/A up to energies beyond TeV/A. This capability is provided by a modified version of the RQMD 2.4 code of H. Sorge [4] for inelastic interactions from 100 MeV/A up to 5 GeV/A, and the DPMJET codes [5] for energies above 5 GeV. Versions of FLUKA running DPMJET II.5 have been available for some time and more recently the current versions of FLUKA are released with DPMJET III embedded. As already noted, the photonuclear disintegration for inelastic interactions of heavy ions have been included in the standard release.

This inherent capability to include the complete heavy ion transport physics has allowed FLUKA to be able seamlessly to simulate the space radiation environment. It is clear from efforts to support detailed space applications that such complete integrated treatments of the physics is absolutely necessary to provide the proper evaluation of the complex radiation environment within spacecraft. This is especially true when addressing the task of evaluating the dose related risks to crew members.

BME Implementation Below 100 MeV/A

Several significant improvements have been implemented since the last report. These include the initial efforts to extend the heavy ion inelastic interaction simulation capability down to threshold from the prior lower limit in RQMD applicability at 100 MeV/A. This has been done by the embedding of selected event generating capabilities based on the Boltzmann Master Equation (BME) theoretical approach [6]. At present, the implemented BME database includes incident ^{12}C and ^{16}O ions, primarily, and for a selection of companion interacting nuclides. More nuclide pairs will be added in the near future.

Beyond just providing general completeness in FLUKA's capabilities, the motivation to extend the treatment of heavy ion interactions to these near threshold energies comes from the need to simulate stopping heavy ion beams that are employed in radiation therapy. Similarly, the need exists in the space radiation simulation application for the accurate treatment of the dose calculations from incident heavy ions that range inside the body.

At low energies (below 100 MeV/A), the Boltzmann Master Equation (BME) theory describes the pre-equilibrium de-excitation of the composite system created by the complete or incomplete fusion of the projectile and target. The thermalization process is assumed to run via nucleon--nucleon scatterings and emissions into the continuum of single nucleons and clusters produced by nucleon coalescence. In this approach, one has to solve a set of coupled differential equations, the numerical integration of which provides the double differential multiplicity spectra of the emitted particles, including several different clusters.

The interfacing problem has been confronted applying the BME theory to complete fusion of a few representative ion pairs at different energies, carrying out a proper parameterization of the resultant ejectile total multiplicities and spectra, and creating a database of the obtained parameters. This way the pre-equilibrium emissions in complete fusion events (the complete fusion probability is evaluated as a function of the incident energy and the mass and atomic numbers of the interacting nuclei) can be calculated, and the final de-excitation of the remaining equilibrated nucleus is handled by the FLUKA evaporation/fission/fragmentation module

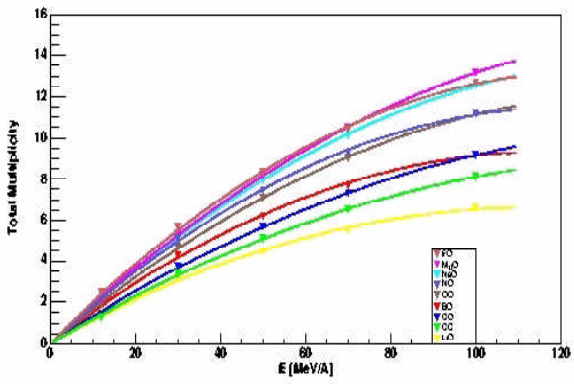

Figure 2. The total multiplicities for some of the complete fusion reactions implemented are shown for the range of incident lab energies from threshold up to 100 MeV/A

For more peripheral collisions, the impact parameter, b, is chosen according to the differential expression of the reaction cross-section $d\sigma_R/db$, which we improved upon over the formula proposed by P.J. Karol [7]. In this approach, a three body picture of the reaction quite naturally follows, envisaging the production of rather cold projectile-like and target-like nuclei, and a middle system preferentially excited, the mass number of which is obtained integrating the projectile's and target's Fermi densities over their overlapping region. At high impact parameters, this reaction mechanism smoothly develops into a sort of inelastic scattering.

This interface is very new and is still undergoing extensive testing in order to crosscheck the results against experimental data and to fine tune its performance. Figure 2 shows the total multiplicity distributions in complete fusion reactions from threshold up to 100 MeV/A for a number of the implemented nuclide pairs.

A New QMD Model

A new QMD model has been developed by our group in the last few years and its interface to the FLUKA code is under development [8], At present, only single ion-ion collision events, without accounting for re-interactions, can be simulated. The fast stage of each reaction is described by the QMD code, while fragment de-excitation by evaporation, Fermi break-up or fission is simulated through other models already embedded in FLUKA routines. De-excitation by photon emission is included too.

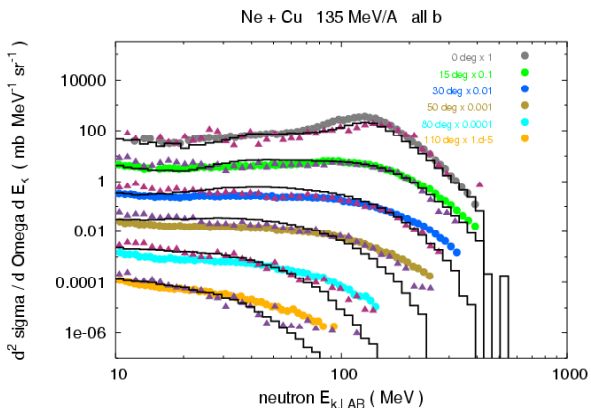

Figure 3. Ne + Cu double differential (in energy and angle) neutron production cross-section at 135 MeV/A bombarding energy. The experimental data, shown by filled dots, are taken from Ref. 10. The results of the theoretical simulation, performed by our QMD + FLUKA, for neutron emission at different angles (0, 15, 30, 50, 80, 110 deg), scaled by a factor 1, 10^{-1}, 10^{-2}, 10^{-3}, 10^{-4} and 10^{-5}, respectively, to distinguish them on the same plot, are shown by triangles. We emphasize that there has not been any normalization factor applied to these results. New QMD results can be compared to those obtained by RQMD + FLUKA, shown by solid lines.

Preliminary results concerning charge yield distributions and double-differential neutron production cross-sections have been obtained [9]. The results from C and Ne ion beams hitting thin targets of C, Al and Cu at 135 MeV/A bombarding energy have been compared to the published experimental data [10], showing a good overall agreement, and to the results of other theoretical simulations, performed with the existing RQMD + FLUKA interface. The new QMD code has been developed in order to improve the accuracy and the self-consistency of the heavy ion event generator at intermediate energies with the other FLUKA models [11]. Energy conservation and initial hot-stage fragment definition come directly from the model, and protons and neutrons are fully distinguished both in terms of mass and in terms of isospin. An example of the performances of this model at present is shown in Figure 3.

Recent Measurements and the RQMD-DPMJET Cross Over Energy

RQMD and DPMJET handoff between each other at 5 GeV/A, and it is of course desirable that the outputs of these event generators blend seamlessly together in their overall predictions at this energy. There is currently some disagreement between the detailed outputs of these two event generators in the overlap region as is demonstrated in their predictions shown in Figure 4.

In order to address this discrepancy data were taken for common fixed beam rigidities at each of the nominal beam settings at ~3, 5 & 10 GeV/A. At each energy setting, a sequence of 3 different beams was supplied, C, Si and Fe. The same sequence of elemental target materials were employed for each beam energy/species combination and their thicknesses were adjusted to maintain ~ 0.5 interaction lengths in each case. The elemental targets consisted of C, Al, Fe and Cu.

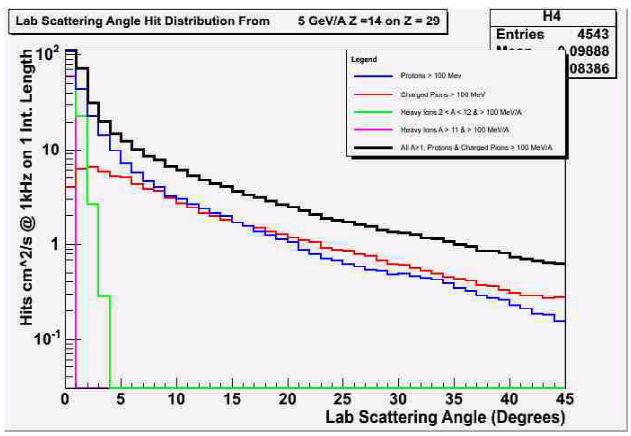

Figure 4a

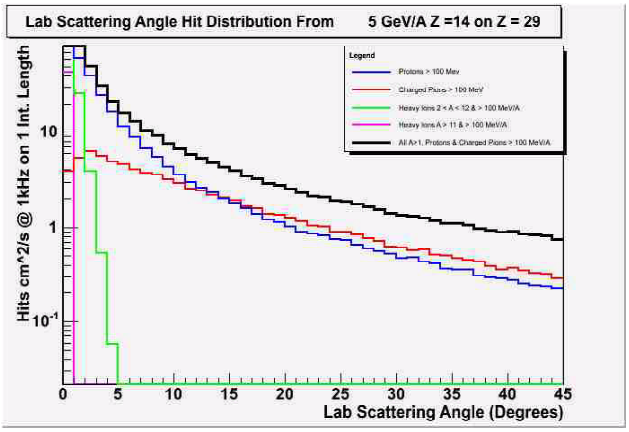

Figure 4b

Figure 4. The predictions for the lab scattering angles from DMPJET 3.0 (3a) and RQMD (3b) for 5 GeV/A Si Beam incident on Cu. Note the differences in the light ions (green). Protons (blue) and Pions (red).

Figure 5 shows a preliminary plot of raw hits from strip detectors which were arrayed in a fan from 3-45 degrees on either side of the beam centreline as a function of the scattering angle as measured from the center of the target. Superimposed on the raw data is an arbitrarily normalized prediction from the current version of FLUKA. This simulation was done using FLUKA in its standard configuration wherein both of the event generators (RQMD & DPMJET-III) in the Monte Carlo runs were used as mutually exclusive alternatives randomly selected using a linear crossover scheme stretched over the 4-6 GeV/A range. In this scheme, RQMD starts out at 4 GeV/A being used 100% of the time, linearly decreasing in probability to 0% at 6 GeV/A, with DPMJET-III doing the opposite.

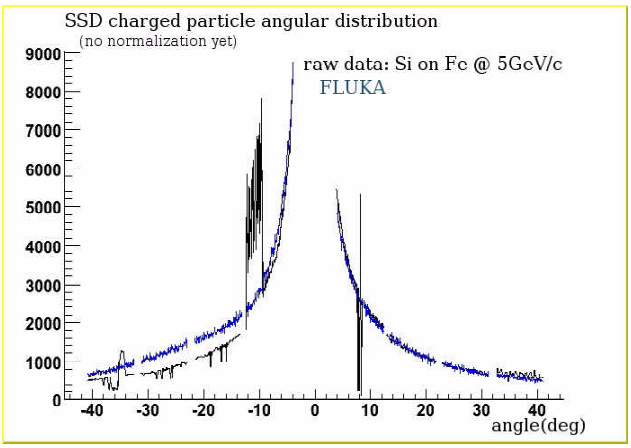

Figure 5 – The raw data are shown in black for 5 GeV/A Si incident on an Fe target. The FLUKA results, arbitrarily normalized, are shown in blue. Some noisy channels are clearly evident. The asymmetry is due to a slight offset in the detector.

The Application of FLUKA to Proton Therapy Treatment Planning and PET Monitoring

At Massachusetts General Hospital, Boston, MA, USA, the feasibility and potential of PET/CT (positron emission tomography/X-ray computed tomography) imaging for treatment verification starting within 15-20 min. after proton irradiation is currently under investigation. The physical principle is the production in tissue of positron emitters such as ^{11}C (half-life $T_{1/2}$=20.4 min.) along the proton beam penetration as a by-product of irradiation. These positron-emitting isotopes resulting from target fragmentation of the irradiated nuclei can be potentially visualised by PET imaging as a spatial marker of radiation dose deposition. The pattern of produced positron-activity is however not directly proportional to the delivered dose because of the different nuclear and electromagnetic processes. A possible approach for treatment verification which is for example pursued at GSI Darmstadt, Germany, for carbon ion therapy requires Monte Carlo techniques for calculating the PET image expected on the basis of the treatment plan [12]. The comparison with the measured activity distribution provides valuable information on the correct delivery of the prescribed treatment [13]. For this purpose, a calculation tool for prediction of proton induced positron-activity was developed using the FLUKA code, internally combined with experimental cross-sections as described in [14]. The latter approach was however extended to include further reaction channels leading to the main long-lived positron-emitters detectable with the used off-line imaging technique, i.e. with a detector located outside the treatment site. The input phase space of the proton beam, which is shaped using passive devices, is provided by a Geant4-based Monte Carlo simulation modelling the entire nozzle of the beam delivery [15]. Whereas calculations for phantom experiments can be based upon standard combinatorial geometry description, simulations in patients were performed using the raw CT scans. Conversion of the Hounsfield Units (HU) into mass density and elemental composition was based on the work of Schneider et al[16]. This basically segments the CT scan into 24 main materials. The HU-dependent adjustment of electromagnetic and nuclear processes for these 24 materials sharing the same composition and a nominal mean density was accomplished by means of additional scaling factors as proposed in [17], using the experimental ``CORRFACT'' option recently implemented in FLUKA. This scaling formalism furthermore allows one to adjust the ionization processes to reproduce the same HU-relative stopping power calibration curve typically used by treatment planning programs in charged hadron therapy [18]. Results obtained in phantom experiments and clinical studies will be soon reported in two separate papers. Figure 6 illustrates the good agreement between the prescribed dose distribution in a patient calculated by the commercial treatment planning system FOCUS/XiO (Computerized Medical Systems Inc.) in clinical use at Massachusetts General Hospital and by FLUKA using the described approach.

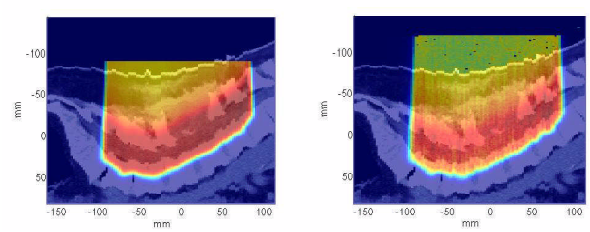

Figure 6. Planned dose distribution calculated using the FOCUS/XiO treatment planning system (left) in comparison to the FLUKA prediction (right) for a postero-antero irradiation of a patient with a tumour in the lower spine. The difference in the entrance channel is because of the different spatial region for which the dose data were saved.

Progress On A GUI-Based Front-End

Work has progressed towards the release of a GUI-based front end interface to allow the user to assemble the standard FLUKA input file in an automated GUI environment. The interface will be linked to the manual to allow rapid access to the reference information for each of the input choices. In addition, a logical cross checking feature will advise the user when separate input options tend to conflict or when it is not generally advisable to simultaneously employ both. The geometry input is intended to be contained in a separate file, which can be created in another GUI environment as described in the next section, and imported to the Front End GUI to allow its use in setting up the other options.

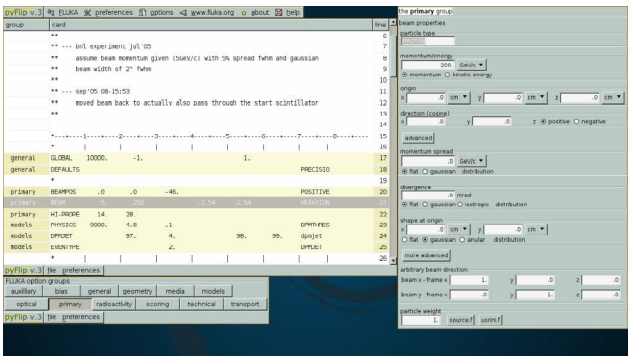

Figure 7. A Screen shot of the beta version of the GUI-base Front End for FLUKA.

The Front-End interface is being developed using python as the underlying high-level programming environment. Ultimately, the intention is to produce an XML-based version. A beta version of the interface is currently undergoing testing and is depicted in Figure 7.

SimpleGeo, As a Geometry Creation Tool for FLUKA

Work has progressed towards the release of a GUI-based geometry creation tool based on the SimpleGeo interface. Figure 8 shows a Screen shot of this interface.

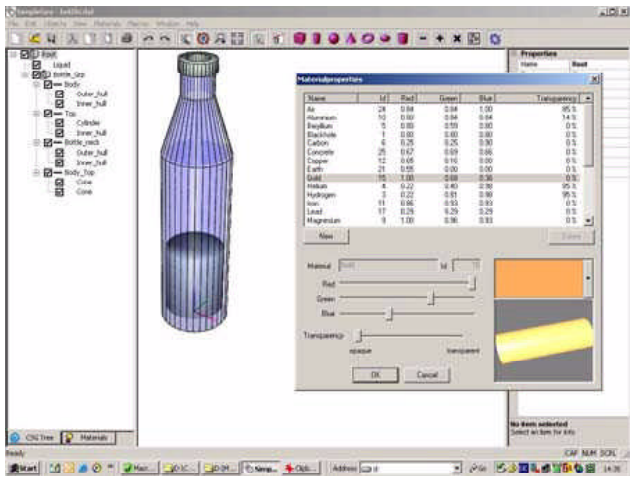

Figure 8. A screen shot of the SimpleGeo interface. This tool allows users to both create and visualize geometries in a full-featured elegant CAD-like GUI environment and export the output in a file that can be directly employed by a standard FLUKA input file.

Acknowledgements

This work is supported in part by NASA grants NGR8-1658 & NGR8-1901, by DOE (contract number DE-AC02-76SF00515) and by EC (contract no. FI6R-CT-2003-508842, "RISC-RAD"), as well as by the Institute for Space Operations at the University of Houston.

References

[1] L. Pinsky, *et al*., CHEP-2004-paper 280, Interlaken, Switzerland, 30 Sep. – 1 Oct. 2004, A. Fassò, et al., CHEP-2003-MOMT004, CHEP 03, La Jolla, California, 24-28 Mar 2003. Published in **eConf C0303241:MOMT004,2003**.

[2] D.E. Cullen, J.H. Hubbell and L. Kissel, *EPDL97: The Evaluated Photon Data Library*, '97 Version UCRL--50400, Vol. **6**, Rev. 5 (1997).

[3] G. Marsaglia and W. W. Tsang., Statistics Probability Letters, **66**, 183--187 (2004)

[4] H. Sorge, et al., Ann. of Phys. **192**, 266, (1989).

[5] S. Roesler, R. Engel and J. Ranft, Proc. of Monte Carlo~2000 Conf., Lisbon, October 2000, Springer-Verlag Berlin, 1033 (2001); and J.Ranft, Phys. Rev. **D51**, 64 (1995).

[6] M. Cavinato, E. Fabrici, E. Gadioli, E. Gadioli Erba, and G. Riva, Nucl. Phys., **A679**, 753-764 (2001).

[7] P.J. Karol, Phys. Rev. **C11** (1975) 1203, and F. Cerutti, A. Clivio, and E. Gadioli, Eur. Phys. J. **A25**, 413 (2005).

[8] A. Fasso`, A. Ferrari, J. Ranft and P.R. Sala, *CERN Yellow Report*, 2005-10 (2005), INFN TC 05/11.

[9] M.V. Garzelli, F. Ballarini, G. Battistoni, poster presented at NPDC 19, Pavia, Italy, September 5 - 9 2005; submitted to the IOP Journal of Physics, Conference Series.

[10] H. Sato, T. Kurosawa, H. Iwase, et al., Phys. Rev. **C64**, 034607-1,12 (2001).

[11] H. Aiginger, et al., Adv. Space Res. **35**, 214 (2005).
[12] F. Ponisch, K. Parodi, B.G. Hasch and W. Enghardt, Phys. Med. Biol. **49**, 5217-32 (2004).
[13] W. Enghardt, P. Crespo, F. Fiedler, R. Hinz, K. Parodi, J. Pawelke and F. Ponisch, Nucl. Instrum. Medhods A, **525**, 284-8 (2004).
[14] K. Parodi, W. Enghardt and T. Haberer, Phys. Med. Biol., **47**, 21-36 (2002).
[15] H. Paganetti, H. Jiang, S-Y. Lee and H. Kooy, Med. Phys., **31**, 2107-18 (2004).
[16] W. Schneider, T. Bortfeld and W. Schlegel, Phys. Med. Biol. **45**, 459-78 (2000).
[17] H. Jiang and H. Paganetti, 2004 Med. Phys., **31**, 2811-8 (2004).
[18] L. Hong, M. Goitein, M. Bucciolini, R. Comiskey R, B. Gottschalk, S. Rosenthal, C. Serago and M. Urie, Phys. Med. Biol., **41**, 1305-30 (1996)